Carbohydrate Polymers 101 (2014) 136–145

Contents lists available at ScienceDirect

Carbohydrate Polymers

journal homepage: www.elsevier.com/locate/carbpol

Interactions between carboxymethyl konjac glucomannan and soy protein isolate in blended films

Le Wang[a], Man Xiao[a], Shuhong Dai[a], Jia Song[a], Xuewen Ni[a], Yapeng Fang[a,b], Harold Corke[a,c], Fatang Jiang[a,*]

[a] Glyn O. Philips Hydrocolloid Research Centre at HUT, Hubei University of Technology, Wuhan 430068, China
[b] Glyn O. Philips Hydrocolloid Research Centre, Glyndwr University, Plas Coch, Mold Road, Wrexham LL11 2AW, United Kingdom
[c] School of Biological Sciences, The University of Hong Kong, Hong Kong, China

ARTICLE INFO

Article history:
Received 18 March 2013
Received in revised form 7 September 2013
Accepted 10 September 2013
Available online 14 September 2013

Keywords:
Carboxymethyl konjac glucomannan
Soy protein isolate
Blending
Biopolymer interactions

ABSTRACT

To elucidate biopolymer interactions between carboxymethyl konjac glucomannan (CMKGM) and soy protein isolate (SPI) in different ratios on physicochemical properties of the blended films, biodegradable CMKGM/SPI films were prepared and characterized.

The results showed that CMKGM and SPI are highly compatible in blended film formation, and that Maillard reactions and hydrogen bonds interactions between CMKGM and SPI occurred. The water adsorption of the CMKGM/SPI films progressively decreased with increasing CMKGM level, the surface wettability of the blended films was improved with increasing CMKGM content; the CMKGM/SPI blend films had enhanced tensile strength (TS) and elongation at break (EAB) compared to pure CMKGM and SPI films; the oxygen permeability of blend films was decreased; the roughness was decreased with increasing CMKGM content. Moreover, the CMKGM/SPI film was biocompatible and biodegradable.

1. Introduction

With the long term and increasing trend to reduce the environmental impact caused by human activities, special attention is being paid to explore renewable biopolymer-based materials to replace conventional petroleum-based materials (Siracusa, Rocculi, Romani, & Rosa, 2008). Biopolymer-based materials are therefore widely studied in academia and industry because of these environmental concerns as well as the costs and supply limitations of petroleum (Jansson, Järnström, Rättö, & Thuvander, 2006; Yu, Dean, & Li, 2006).

Although considerable work has been done in development of protein films as biodegradable packaging materials in recent years, and despite the excellent gas barrier properties of protein films, they tend to have higher water vapor permeability, mechanical weakness and lower elongation as compared to the best synthetic polymers (Wihodo & Moraru, 2012).

Soy protein is a plant protein with many potential applications due to its relatively low cost, wide availability, and complete biodegradability. In particular, soy protein isolate (SPI), with higher protein content than other soy protein products, has superior film-forming ability (Rhim, 2007) and excellent oxygen permeability (Song, Tang, Wang, & Wang, 2011). Nevertheless, SPI film is not widely used commercially, due to its poor mechanical properties and relatively high moisture sensitivity (Rhim, 2004). To improve these properties of SPI-based materials, different modification methods have been performed on it, such as physical (Kyung Kim, Jo, Jin Park, & Woo Byun, 2008), enzymatic (Tang, Jiang, Wen, & Yang, 2005) and chemical treatments (Shand, Ya, Pietrasik, & Wanasundara, 2007). Beyond these, blending can be an effective approach to improve the properties of films (Park, Hettiarachchy, & Were, 2000; Rhim, 2007). Carboxymethyl cellulose (Su, Huang, Yuan, Wang, & Li, 2010), waterborne polyurethane (Zhang, Song, Wang, & Wang, 2012), starch (Mariani, Allganer, Oliveira, Cardoso, & Innocentini-Mei, 2009) and gelatin (Denavi et al., 2009) have been blended with SPI to enhance the physicochemical properties of the films.

Carboxymethyl konjac glucomannan (CMKGM), one of the most important derivatives of konjac glucomannan (KGM), is a typical anionic polysaccharide that shows amphiphilic characteristics. CMKGM film has good mechanical properties, water resistance, biocompatibility, good film-forming ability and biodegradability (Zhan et al., 2006).

Abbreviations: KGM, konjac glucomannan; CMKGM, carboxymethyl konjac glucomannan; SPI, soy protein isolate; FTIR, Fourier transform infrared; XRD, X-ray diffraction; DSC, differential scanning calorimetry; SEM, scanning electron microscopy; AFM, atomic force microscopy; EAB, elongation at break; TS, tensile strength; DVS, dynamic vapour sorption.

* Corresponding author. Tel.: +86 027 88021796; fax: +86 027 88021796.
E-mail address: JIANGFT@mail.hbut.edu.cn (F. Jiang).

0144-8617/$ – see front matter © 2013 Elsevier Ltd. All rights reserved.
http://dx.doi.org/10.1016/j.carbpol.2013.09.028

Interactions between biopolymers in the film-forming process, such as for κ-carrageenan and locust bean gum (Martins et al., 2012), quinoa protein and chitosan (Abugoch, Tapia, Villamán, Yazdani-Pedram, & Díaz-Dosque, 2011), and agar, cassava starch and arabinoxylan (Debeaufort, Voilley, & Luu, 2009), have been reported and lead to the changes of physicochemical properties of films, such as mechanical properties, water solubility and water sorption.

SPI and CMKGM (degree of carboxymethylation = 0.618) blend films were reported in our previous article (Tang, Du, Zheng, & Fan, 2003), the results showed that the mechanical properties, thermo stability, and water vapor barrier properties of the blend films were clearly improved after mixing of SPI and CMKGM. Whilst the film has been prepared and characterized, no definitive explanation was proposed as to the fundamental basis for the changes in physicochemical behavior of the blended films.

The general aims of this work were to characterize the effect of the CMKGM/SPI mixture on physicochemical properties of their films and elucidate the mechanism of the biopolymer interactions between CMKGM and SPI in blended films. The novelty is the attempt at a definitive explanation to the changes in physicochemical behavior of the CMKGM–SPI films.

2. Experimental

2.1. Materials

2.1.1. Preparation of CMKGM solution

Konjac glucomannan (KGM) was purchased from Licheng Biological Technology Company (Wuhan, China) and purified by mixing in sequence with three times volume of 50, 75 and 95% (v/v) ethanol for 3 h at 25 °C, followed in each case by vacuum drying at 50 °C for 5 h. Carboxymethyl konjac glucomannan (CMKGM) was prepared following Zhou et al. (2006). KGM (5.0 g) and sodium acetate (30.0 g) were put in a beaker, 50 mL 70% (v/v) ethanol solution was added, it was continuous stirred at room temperature for 60 min, then 3.00 g chloroacetic acid was added with further continuous stirring at 200 rpm at 60 °C. Then the system was washed with 50, 80, 95% (v/v) alcohol separately, and dried in a vacuum oven at 60 °C for 8 h. The degree of substitution (DS) was calculated by the potentiometric titration method (El-Sherbiny, 2009). The degree of acetylation (DA) was calculated following Chua et al. (2012).

Carboxymethyl konjac glucomannan powder (2 g) was put in 100 mL deionized water with continuous stirring at 200 rpm at 60 °C for 3 h, and the CMKGM solution (solution A) was left at 4 °C for 12 h to eliminate bubbles and allow sufficient swelling before use.

2.1.2. Preparation of SPI solution

Soy protein isolate (SPI) powder (moisture content < 5.0%, minimum 90% protein content on dry basis) was purchased from Man Tianxue Company (Henan, China). SPI solution (solution B) was prepared by adding 2.0 g SPI powder to 100.0 g deionized water, and adjusting pH to 10.0 with 2.0 mol L^{-1} NaOH solution, with continuous stirring at 200 rpm at 90 °C for 60 min.

2.2. Blend film preparation

A series of films from blended CMKGM and SPI solutions was prepared. Mixtures of solutions A and B were thoroughly stirred to form the film blend sol. The pH of the blend sol was adjusted to 8.0 with 2.0 mol L^{-1} NaOH solution at 60 °C. The mixed sol, after vacuum defoaming, was poured on a glass plate measuring 12 cm × 12 cm × 1 cm to form film. The glass plate was dried to constant weight in an oven at 60 °C for 8 h. Dried films were removed carefully from the plate surface, and conditioned at 25 ± 1 °C, 50 ± 5% relative humidity for 24 h before testing. A series of CMKGM/SPI blend films coded as CS-m were prepared by controlling the CMKGM and SPI weight ratios, where m is weight percent CMKGM based on the total weight of CMKGM and SPI.

2.3. Characterization

2.3.1. Fourier transform infrared (FTIR) spectroscopy

The IR spectra of pure and blend films were recorded on a Nicolet Nexus 670 spectrometer (Nicolet Instruments, Madison, WI) using DTGS KBR detector and KBR beam splitter for mid-IR (4000–500 cm^{-1}) data collection, and the data were analyzed by Omnic 3.2 software (Nicolet Instruments). All samples were scanned from 4000 to 500 cm^{-1}. Data were collected by averaging 64 scans with resolution 2 cm^{-1}.

2.3.2. X-ray diffraction (XRD)

The structural properties of films were characterized by an X-ray diffractometer (XRD, D8 Advance, Bruker, Karlsruhe, Germany) equipped with Cu Kα radiation (λ = 0.1542 nm). The scan data were collected in the 2θ range of 2–50° at 10° min^{-1} scan rate.

2.3.3. Differential scanning calorimetry (DSC)

Thermal properties of films were obtained with a Mettler Toledo DSC 1 (Mettler Toledo, Zurich, Switzerland) device, operating with STARe software version 10.00. The samples (5 mg) were hermetically sealed in aluminum pans and heated at a rate of 10 °C min^{-1} from 30 to 250 °C under a N_2 atmosphere.

2.3.4. Surface morphology

The films were attached using double face adhesive tape and were then gold-sputter-coated. The microstructure of the films was observed by scanning electron microscopy (SEM, JSM-6390LV, JEOL Ltd., Tokyo, Japan).

The topography of the films was obtained using a Digital Instruments atomic force microscope (DI Nanoscope TV, Veeco Company, Plainview, NY) equipped with an E-scanner. Tapping mode with nominal spring constant of 20–100 N m^{-1} and nominal resonance frequencies of 10–200 kHz were employed. The instrument was operated in tapping mode with topography scan size in the range 2 μm × 2 μm to 20 μm × 20 μm. The software NanoScope v 5.31r1 (Veeco, USA) was used to calculate the roughness value of the films.

2.3.5. Adsorption isotherms

The water adsorption isotherms of the films were determined using a DVS Intrinsic apparatus (Surface Measurement Systems, London, UK). The 5 mg sample was exposed to a relative humidity (RH) range from 0 to 95% (RH = 10, 20, 30, 40, 50, 60, 70, 80, 90 and 95%, respectively) until the sample reached equilibrium. All measurements were performed at 25 °C.

DVS method has high data reproducibility and can provide accurate isotherms at any desired relative humidity (0–95%) with short measurement time at different pre-set isotherm temperatures, highly reproducible data using this DVS technique was generated (Hill, Norton, & Newman, 2009), so only one measurement was carried out for each sample.

2.3.6. Wettability

Wettability of films with dimensions of 4.0 cm × 4.0 cm was evaluated from the contact angle measurement of water droplet deposited on the film surface using a G1 Krüss goniometer (KRÜSS GmbH, Germany) equipped with a CCD camera and an image analysis software (Drop Shape Analysis, KRÜSS, Germany). Contact angle was determined at 25 °C and expressed in degrees.

2.3.7. Mechanical properties

Film samples were equilibrated at 25 ± 1 °C, 50 ± 5% relative humidity (RH) for 3 days before testing. Film thickness (mm) was measured by a micrometer (Shanghai Liu-ling Instrument Company, Shanghai, China) at eight random points of film testing area. The average thickness of the films was used for the determining mechanical and barrier properties. The tensile mechanical properties were determined using a texture analyzer (TMS-Pro, Food Technology Corporation, Hampton, VA). Tensile strength (TS) and percent elongation at break (%*E*) were measured according to the ASTM standard method D882-91 (ASTM-D-882-91, 1991). Films were cut into 10 mm × 50 mm strips and clamped between grips, leaving an initial length 35 mm between the grips. The test speed was set at 12 mm min^{-1}. TS was expressed in MPa and calculated by dividing the maximum load (N) by the initial cross-sectional area (m^2) of the strips. Elongation at break was determined as the ratio of the final length at the point of sample breakage to the initial length of a specimen (35 mm) and multiplying by 100.

2.3.8. Oxygen permeability

The oxygen permeability (OP) of the films was tested by a gas permeability tester (VAC-V1, Labthink Instruments, Jinan, China) according to the Chinese National Standard of GB/T 1038-2000.

The films with 50 mm × 50 mm were sealed between two chambers. All the chambers were evacuated initially. Then one chamber with O_2 at a specific high pressure, the other chamber at a lower pressure, oxygen diffused through the film into the lower pressure chamber. The oxygen transmission was indicated by pressure changes. The samples were tested at 23 ± 1 °C and a relative humidity of 50 ± 1%. The oxygen permeability (OP) of the films was calculated by Eq. (1).

$$\mathrm{OP} = \frac{\Delta p}{\Delta t} \times \frac{V}{S} \times \frac{T_0}{p_0 T} \times \frac{24}{p_1 - p_2} \quad (1)$$

where OP is the oxygen permeability (cm^3/m^2 d Pa), $\Delta p/\Delta t$ (Pa/h) is the arithmetic mean of the pressure variation in unit time in the low pressure chamber, V (cm^3) is the volume of low-pressure chamber, S (m^2) is the test area of the film specimen, T (K) is the test temperature, T_0 and p_0 is the temperature under standard conditions (273.15 K) and pressure (1.0133×10^5 Pa), $p_1 - p_2$ is a pressure difference between the 2 sides of film (Pa).

2.3.9. Biocompatibility evaluation

The cytotoxicity assay was measured according to reported methods (Neamnark et al., 2007; Pei et al., 2013).

Briefly, mouse fibroblast cell line L929, obtained from the Type Culture Collection of the Chinese Academy of Sciences, was cultured in Dulbecco's modified Eagle's medium (DMEM, Hyclone, SH30022.01B) supplemented with fetal bovine serum (Gibco, NO. 10099-11) at 37 °C in CO_2 cell incubator (Thermo 3111, Billups-Rothenberg, Del Mar, CA). When the cells of the control and experimental groups in logarithmic phase, they were trypsinized with 0.25% (w/w) trypsin (BYL40926, JRDUN biotechnology, Shanghai). Then cells were diluted to 1–5 × 10^4 cells mL^{-1}, take 100 μL to 96-well culture plates, the cells were cultivated for 12 h at 37 °C. For cell grow study, L929 cells were inoculated into the culture medium with and without films for 12, 24, 48, and 72 h, then the number of cells was determined by MTT assay.

Experimental procedure of MTT assay was as follows: each hole was included 20 μL of 0.5 mg mL^{-1} MTT solution to incubate for 4 h then the culture solution was removed, each hole was added 150 μL DMSO, and set on shaker to oscillated with low speed for 10 min until the crystals was dissolved fully. The absorbance at 490 nm was measured by using Microplate Reader (Thermo Multiskan MK3, Thermo Lab-systems, Vantaa, Finland). The intensity of the absorbance is proportional to the number of living cells.

2.3.10. Biodegradability

Biodegradability of the films was tested by inoculating the films with *Aspergillus niger* according to the reported method (Alves et al., 2011). Briefly, *A. niger* (CGMCC 3.3928) were obtained from China General Microbiological Culture Collection Center. The potato dextrose agar media was potato 80 g, glucose 4 g, distilled water 400 mL, agar 2 g/100 mL. The agar surfaces were cultivated with *A. niger*, then the films (2.0 cm × 2.0 cm) were faced on the surface of agar in a Petri dish. After 15 days at 25 °C, the films were examined for evidence of colony growth.

2.3.11. Statistical analysis

All experiments described above except for the determination of adsorption isotherms without repeat test were made in triplicate for each sample. One-way analysis of variance (ANOVA) was used to examine differences between means. Tukey's multiple range test ($p < 0.05$) was applied to detect significant differences among means. The statistical analysis was performed using SPSS version 13.00 for Windows (SPSS, Chicago, IL).

3. Results and discussion

3.1. The characteristics of CMKGM and CMKGM/SPI film

The degree of substitution (DS) of the carboxymethylated KGM was 0.29. The weight percent of acetyl-substituted residues in the KGM and CMKGM backbone was 1.65% and 0.86%, respectively.

In previously published reports, CMKGM was prepared in aqueous alkaline solution using monochloroacetic acid under the catalytic action of sodium hydroxide or potassium iodide (Kobayashi, Tsujihata, Hibi, & Tsukamoto, 2002; Niu, Wu, Wang, Li, & Wang, 2007), and alkaline deacetylation reaction of KGM occurred in aqueous alkaline solution (Chen, Li, & Li, 2011). Deacetylation of KGM changed its structure from a semi-flexible straight chain into an elastic microsphere with greatly reduced inherent viscosity and increased asymmetry (Wang, Li, & Xie, 2005). The presence of acetyl groups confers solubility on KGM in aqueous solution (Du, Li, Chen, & Li, 2012).

In order to prepare carboxymethyl konjac glucomannan (CMKGM) while retaining acetyl groups, this study adopted a novel method to prepare CMKGM with sodium acetate and chloroacetic acid, successfully preparing CMKGM with 52% acetyl retention. CMKGM with retained acetyl showed special physicochemical properties, and the structure and mechanical properties of the CMKGM/SPI films differ with different degrees of carboxymethylation of CMKGM. Compared to the films prepared by SPI and CMKGM with degree of carboxymethylation 0.29, SPI/CMKGM films with higher degree of carboxymethylation of CMKGM cannot be formed, while using a lower degree of carboxymethylation of CMKGM, the CMKGM/SPI film was too water sensitive (data not shown). So the CMKGM with degree of carboxymethylation 0.29 was chosen to prepare film with SPI for this study.

3.2. Analysis of interactions between CMKGM and SPI

The chemical structure of CMKGM with degree of substitution 0.29 and the FTIR spectrum of its film (Fig. 1a and d), indicate that the significant broad absorption bands seen at 3400–3200 cm^{-1}, 3000–2800 cm^{-1} and 1100–1300 cm^{-1} are attributable to O—H, C—H, and C—O—C stretching vibration respectively. Also, the absorption band at 1732–1600 cm^{-1} due to the C=O stretching vibration indicates the CMKGM exists as a carboxylate. These absorption bands are in accordance with previous studies (Zhan et al., 2006). The pure SPI film spectrum (Fig. 1b) shows an absorption band at 3302–3150 cm^{-1} revealing the stretching vibration

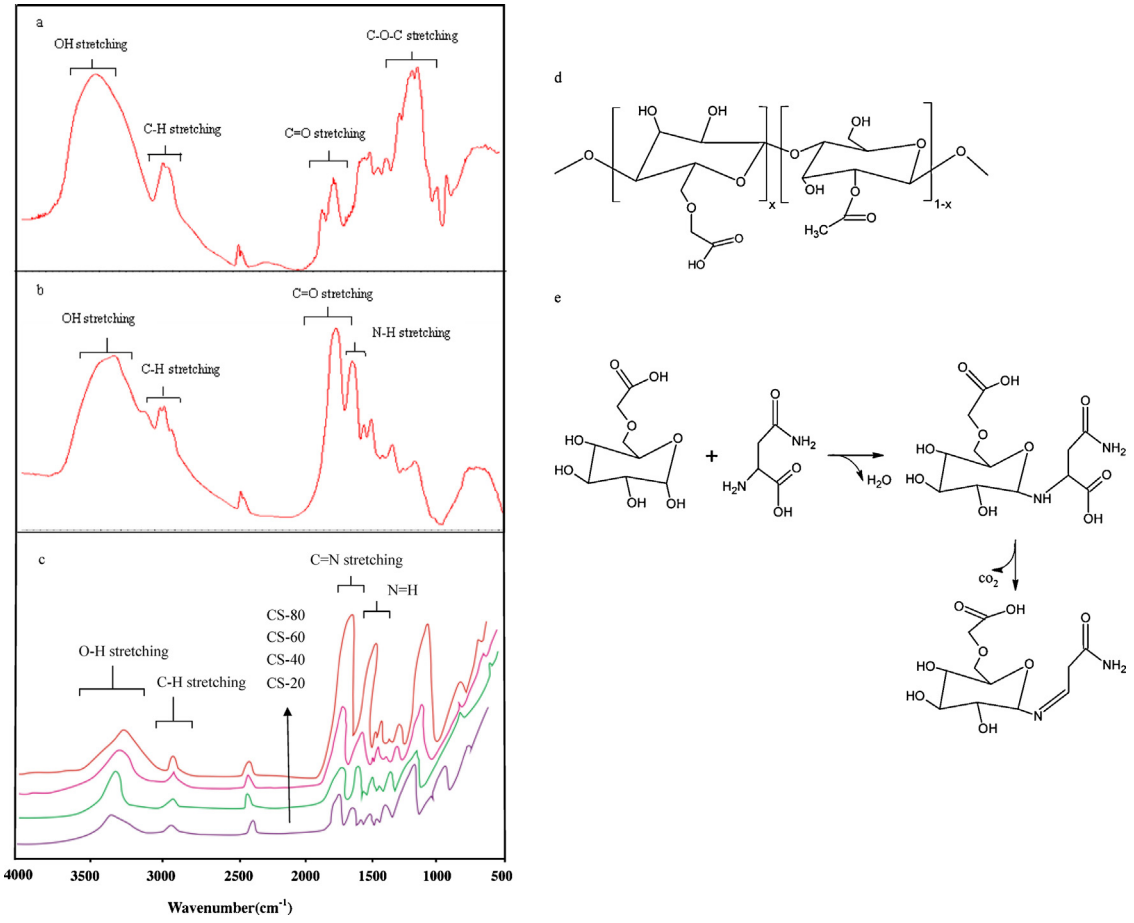

Fig. 1. FTIR of pure CMKGM (a), FTIR of pure SPI (b), FTIR of CS-20, CS-40, CS-60 and CS-80 CMKGM/SPI blend films (c), molecular structure of CMKGM with degree of substitution 0.29 (d), a typical Maillard reaction between CMKGM and an amino acid (glutamine, gln) (e). CS-m refers to the blend ratio, where m is weight percent CMKGM based on the total weight of CMKGM and SPI.

of the —OH group, which can be attributed to hydrogen bonding between protein chains and to moisture in the protein. The absorption bands at 1630–1710 cm^{-1} and 1590–1520 cm^{-1} are assigned to the amide I and amide II bands of SPI, respectively. These absorption bands had been reported for soy protein in previous studies (Abugoch et al., 2011). SPI possesses many reactive side groups, such as —NH_2, —OH, and —SH, which can easily participate in crosslinking reactions. These proteins can react with each other to form crosslinks (Su et al., 2010). FTIR spectra of CMKGM/SPI blend films with various weight ratios (Fig. 1c) show that the intensity of the bands gradually decreased at 1603 cm^{-1} and 1586 cm^{-1}, indicating that the amide I and the amide II stretching vibration peak were diminished with increased level of SPI in the blend. The O—H stretching vibrations at ~3300 cm^{-1} also significantly weakened and shifted gradually to a lower band with the increase of SPI content in the blended films. This indicated that strong hydrogen bonding interactions between CMKGM and SPI in the composites formed during the blending and film-forming process. This suggests that during the blending process at 60 °C, the —OH group in CMKGM and amino groups in SPI reacted together. The C=N stretching vibration at 1638 cm^{-1} appeared in the blend films. Those results may be due to Maillard reaction, in accordance with a previous report (Su et al., 2010). Fig. 1e shows a typical Maillard reaction between carboxymethylated konjac glucomannan and an amino acid molecule (glutamine, gln) (Aaslyng, Larsen, & Nielsen, 1999).

Hydrogen bonding and Maillard reaction interaction between CMKGM and SPI occurred and likely led to changes in films' water sorption, thermal and mechanical properties compared to those of pure CMKGM and SPI film.

3.3. Compatibility analysis between CMKGM and SPI

The XRD of SPI powder shows a characteristic diffraction peak at 2θ 20° (Fig. 2), in agreement with previous reports (Zhang et al., 2012). The CMKGM powder shows a typical diffraction peak at 2θ 22°. The CMKGM/SPI films CS-20, CS-40, CS-60, and CS-80 XRD pattern (Fig. 2) displayed a diffraction peak at 2θ about 22°. The crystallinities of CMKGM, SPI, CS-20, CS-40, CS-60 and CS-80 based on X-ray diffraction were 30.18, 23.72, 19.38, 15.27, and 10.32%, respectively. With increasing CMKGM content in films, the intensity of the diffraction peak of the blend film, compared with CMKGM and SPI, became flatter and broader, which means CMKGM and SPI had good compatibility (Xiao, Liu, Lu, & Zhang, 2001). The crystallinity values of the blend films decreased with increasing CMKGM content, indicating the existence of intermolecular interactions between CMKGM and SPI, which destroyed the original crystalline domains of CMKGM and SPI. The results supported the FTIR analysis conclusion that Maillard reactions between CMKGM and SPI occurred.

The glass transition temperature (*Tg*) is a parameter associated with the system mobility, and is defined as a physical change from the glassy to the rubbery state in amorphous materials promoted by heat (Roos & Karel, 2006). *Tg* is often used as a criterion to assess the miscibility of the polymer blend: a single transition between *Tg* of the two polymers indicates a good miscibility, whereas separate transitions of the mixture indicates immiscibility of their components (Biliaderis, Lazaridou, & Arvanitoyannis, 1999). From DSC curves of CMKGM and SPI blends (Fig. 3), *Tg* were used to determine the compatibility of the blending by analysis of the endothermic

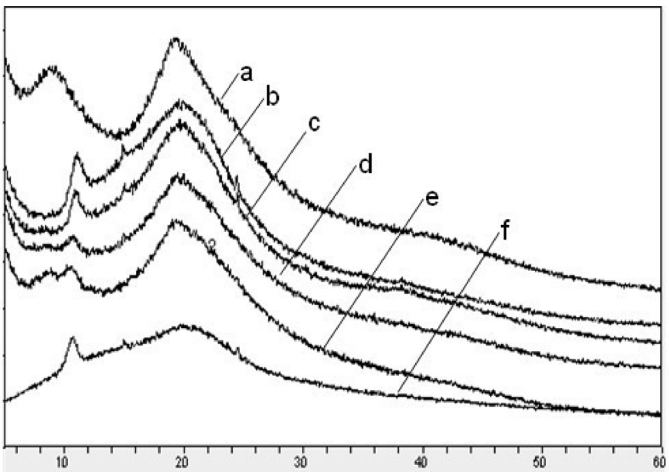

Fig. 2. X-ray patterns of (a) pure SPI powder, CS-20, CS-40, CS-60 and CS-80 (b–e) CMKGM/SPI films, and pure CMKGM powder (f).

peaks from 0 to 250 °C. The DSC curves of pure SPI and CMKGM films showed an exothermic peak at 81.2 and 149.0 °C respectively, corresponding to the respective *Tg*. CMKGM with the degree of carboxymethylation 0.45 and 0.618 showed endothermic peaks at about 100 °C (Du, Dai, Liu, & Dankovich, 2006; Tang et al., 2003). The results of our experiment agreed with the reported results (Du et al., 2006; Tang et al., 2003). Su et al. (2010) and Su, Huang, Liu, Fu, and Liu (2007) showed that the *Tg* of dry soy protein isolate is about 60 °C. Denavi et al. (2009) noted two endotherms, at 113 °C and at 137 °C, which corresponded to the denaturation of the 7S (β-conglycinin) and 11S (glycinin) globulins, respectively. These denaturation temperatures were shifted to higher values than those usually expected for dispersions of those proteins (i.e., at only 78 °C and 92 °C, respectively), due to the low water content of the film (Denavi et al., 2009; Hägerdal & Martens, 1976; Mauri & Añón, 2006). Zhang, Mungara, and Jane (2001) reported that moisture content has a crucial role in determination of thermal properties of soy sheets. With increase in moisture content, the

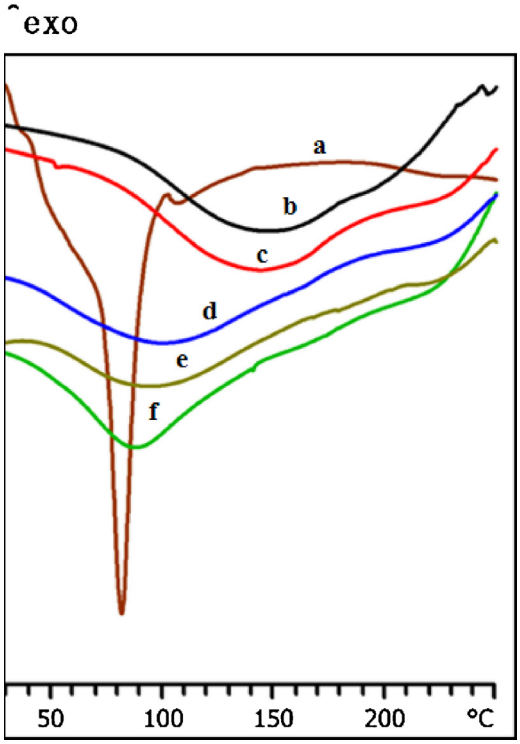

Fig. 3. DSC curves of pure SPI film (a), pure CMKGM film (b), CS-80, CS-60, CS-40, and CS-20 CMKGM/SPI films (c–f).

glass transition temperature of the protein sheets was significantly lowered, reflecting a plasticizing effect of water on the protein network (Zhang et al., 2001). The DSC curves of CMKGM, CS-80, CS-60, CS-40, CS-20 and pure SPI, exhibited exothermic peaks at 149.0, 145.1, 109.8, 102.4, 93.2 and 81.2 °C respectively, corresponding to the respective *Tg*. These endothermic peaks around 80–150 °C were formed by loss of crystalline water. With increasing levels of the CMKGM in the blended films, the *Tg* shifted toward pure of pure CMKGM, i.e., thermal stability of CMKGM/SPI blending films

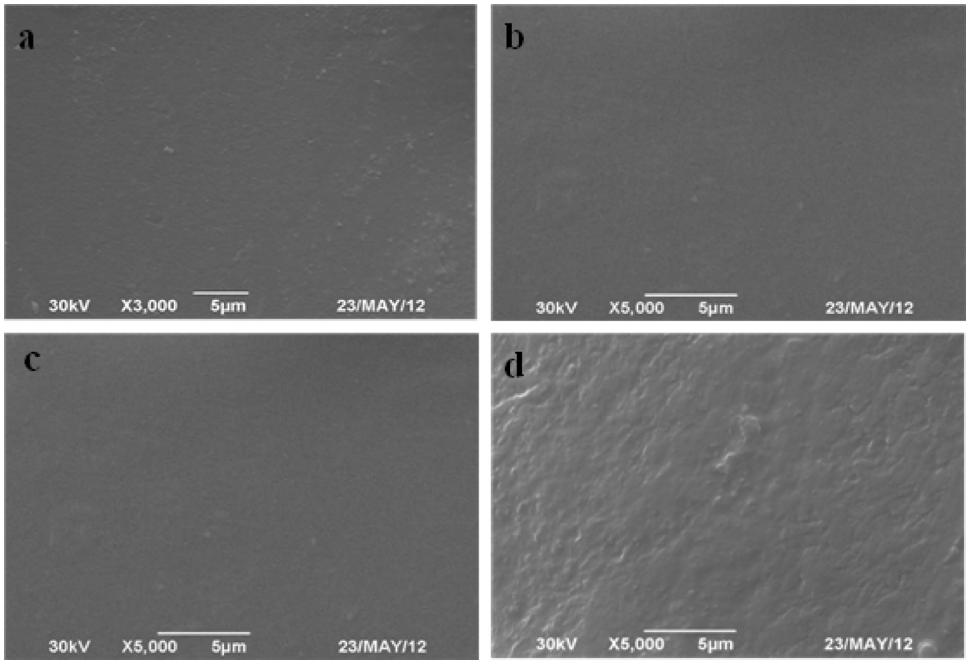

Fig. 4. SEM micrographs of surface of SPI (a), CMKGM (b), surface (c) and cross section of CS-80 (d).

decreased compared with pure CMKGM, but increased compared with pure SPI. The polysaccharide and protein can disrupt their crystalline structures, resulting in the changes of the *Tg*, so forming mutual intermolecular interactions between the blended films. A single *Tg* for the blended polymer system in the DSC heating curves indicates the blends to be miscible and show good compatibility of the component polymers. All blends showed an endothermic peak from 0 to 250 °C, the results suggesting that CMKGM and SPI have good compatibility/miscibility.

The analysis of compatibility of blended films by XRD and DSC indicated intermolecular interactions between CMKGM and SPI formed polymer networks. Compared with the biodegradable films from SPI (Fig. 4a) or CMKGM (Fig. 4b), the blended film (Fig. 4c and d) had a compact, smooth and homogeneous surface without grainy and porous structure, and the cross section had a compact and homogeneous structure, indicating that an ordered matrix was formed, with no layering phenomenon. These results correspond with a previous report (Tang et al., 2003). The microstructure of the films confirmed the compatibility between CMKGM and SPI.

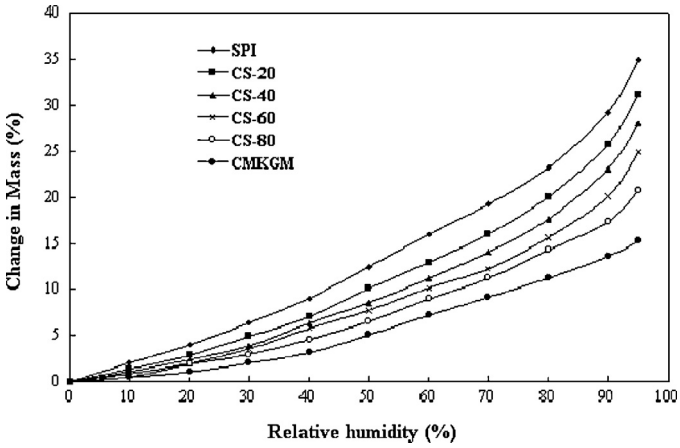

Fig. 5. Moisture adsorption isotherms of pure SPI film, pure CMKGM film, and CS-80, CS-60, CS-40, and CS-20 CMKGM/SPI films at 25 °C.

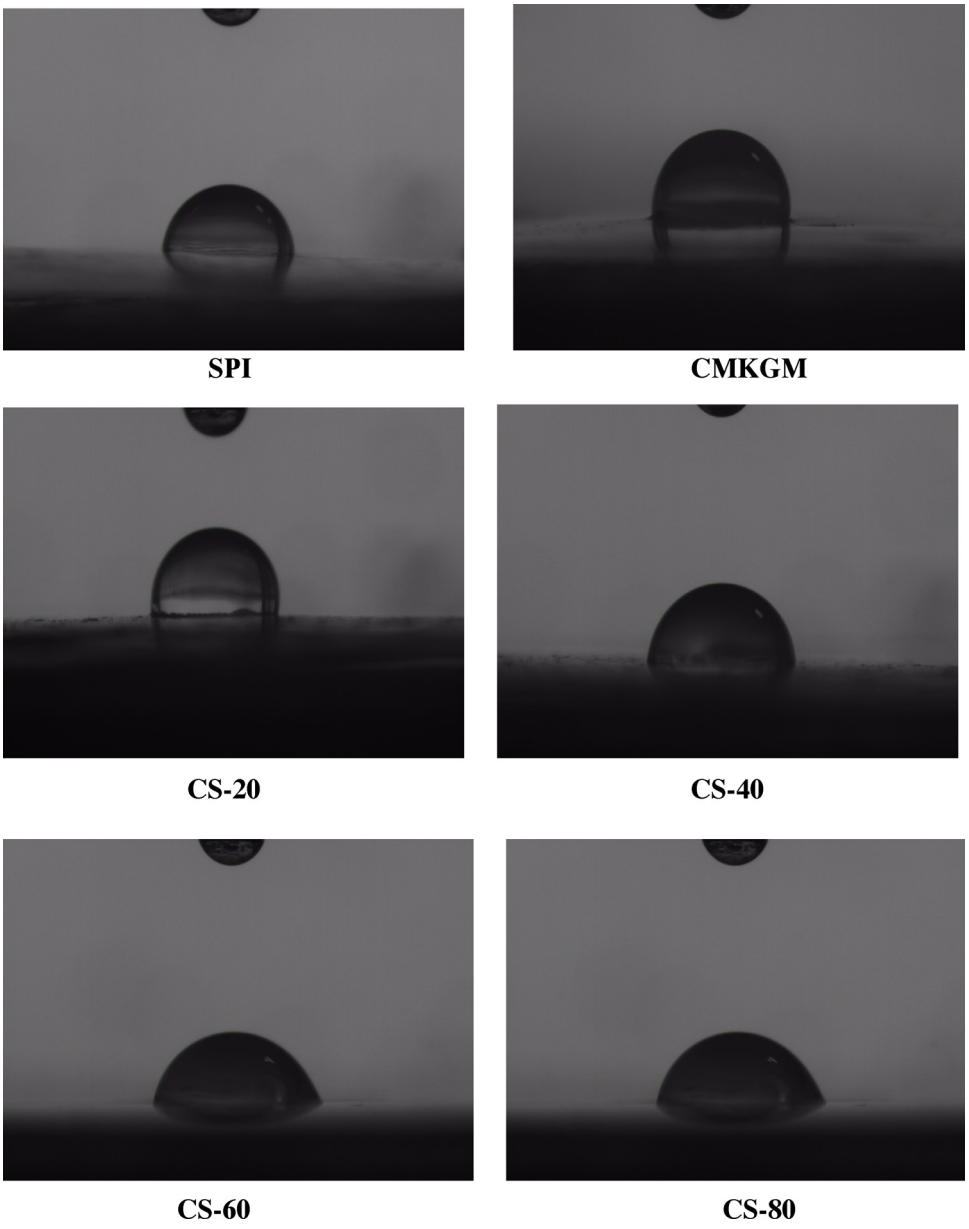

Fig. 6. Contact angle pictures of the films (SPI, CMKGM and CS-m).

Table 1
Contact angle of films prepared from SPI, CMKGM and SPI/CMKGM. Experiments described above were made in triplicate for each sample.

Samples	Contact angles of water (°)
SPI	85.5 ± 2.3[a]
CS-20	86.2 ± 3.2[ac]
CS-40	92.1 ± 3.5[ab]
CS-60	93.3 ± 3.4[e]
CS-80	96.2 ± 4.1[f]
CMKGM	97.3 ± 4.2[b]

Different letters in a column means significant differences at $p < 0.05$.

3.4. Physicochemical properties of CMKGM/SPI films

3.4.1. Adsorption isotherms

Moisture adsorption isotherms of CMKGM/SPI blend films at 25 °C plotted as changes in mass (%) vs. relative humidity (%) (Fig. 5) showed that moisture content increased with increasing relative humidity in all tested films. Pure CMKGM film showed the lowest water adsorption values and pure SPI film had the highest among the tested samples, except at low and high relative humidity. Moisture content of the CMKGM/SPI films under the relative humidity of 0, 10, 20, 30, 40, 50, 60, 70, 80, 90, 95% decreased with increasing contents of CMKGM. This is due to the lower water absorption of CMKGM than SPI; the composite film is not so sensitive to water when the polysaccharide content reaches 80%. This phenomenon is attributed to the polymer hydrophilic group being replaced because of crosslinking reaction and Maillard reactions between CMKGM and SPI. It indicated that blending of CMKGM with SPI changed the microstructure of the films.

3.4.2. Wettability

For the all samples, the CS-80 film showed higher contact angle value, followed by that of CMKGM films (Table 1 and Fig. 6). The contact angle value of the blend films increased with increasing CMKGM content, which indicated that the wettability of the blended films decreased with increasing CMKGM content. CS-80 film surface is the most hydrophobic and SPI is more hydrophilic than CS-80 film surface.

3.4.3. Mechanical properties

The thickness of the films ranged from 0.058 to 0.105 mm (Fig. 7a), and increased with the increasing level of CMKGM in the blend films. The differences in film thickness can be explained by the different film-forming polymer content and the natural properties of the ingredients (Di Pierro et al., 2006). The SPI film had the lowest values of EAB and TS (1.7%, 4.8 MPa) (Fig. 7b and c), similar to a prior report (Kumar, Sandeep, Alavi, Truong, & Gorga, 2010). CS-80 film showed the highest value of EAB and TS (34.9%, 27.3 MPa), which is much higher than those for SPI-based film (11.85%, 2.26 MPa) (Kumar et al., 2010). The EAB and TS of the blend films increased with increasing CMKGM content except for the CS-100 sample, and the maximum values of 34.9% and 27.3 MPa were achieved when the CMKGM content was 80 wt%. The Maillard interactions and hydrogen bonding between CMKGM and SPI could explain these TS and EAB results. The addition of CMKGM to SPI leads to stronger interactions between the two polymers, with a maximum value at the ratio of 80/20 (CMKGM/SPI).

3.4.4. Oxygen permeability

The oxygen permeability of the films was shown in Fig. 8. The OP of CMKGM is highest among all films. When SPI was added to CMKGM film, the value of OP decreased. The value of OP of film was in its lowest when added 20 percent of SPI; this means the barrier of oxygen for CS-80 CMKGM/SPI film is best.

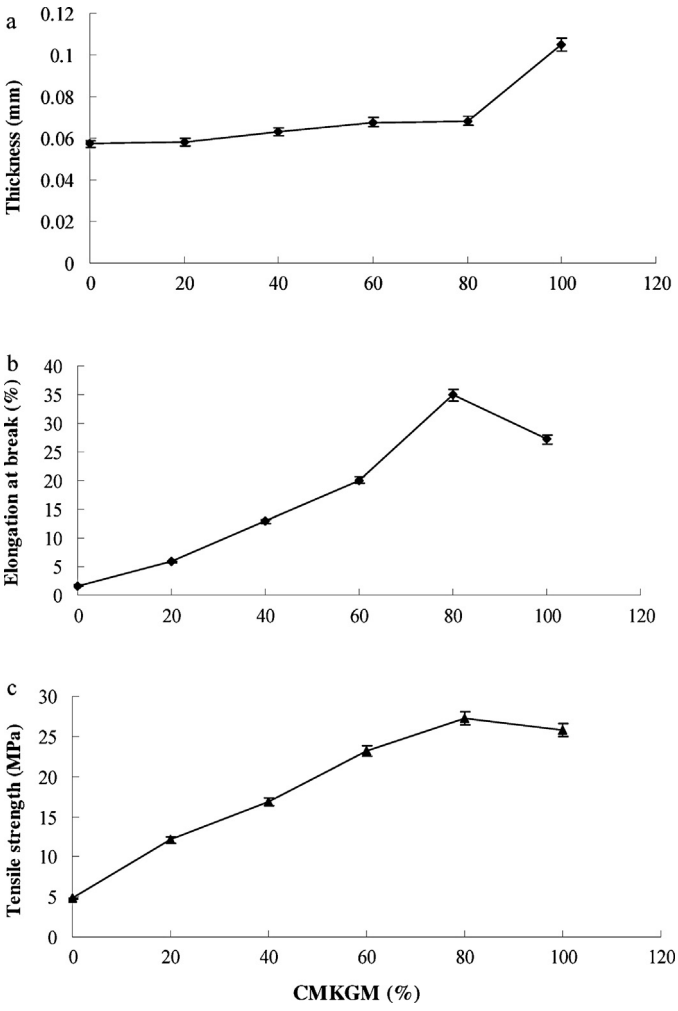

Fig. 7. Thickness (a), elongation to break (b), and tensile strength (c) of composite films as function of weight percent CMKGM based on the total weight of CMKGM and SPI.

The mixture of CMKGM and SPI makes greater molecular interaction, so gives it a tight structure and a low value of OP. It also has been observed that the OP value strongly depends on the interaction between the polymer matrix and O_2 (García, Martino, & Zaritzky, 2000).

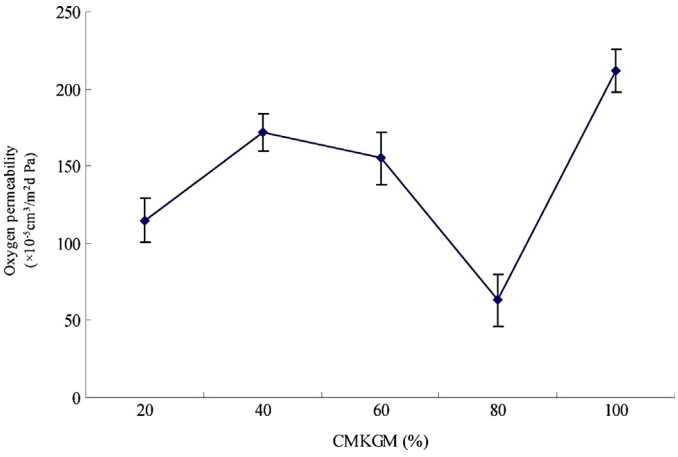

Fig. 8. The oxygen permeability of the CS-20, CS-40, CS-60, CS-80 CMKGM/SPI films, and pure CMKGM film.

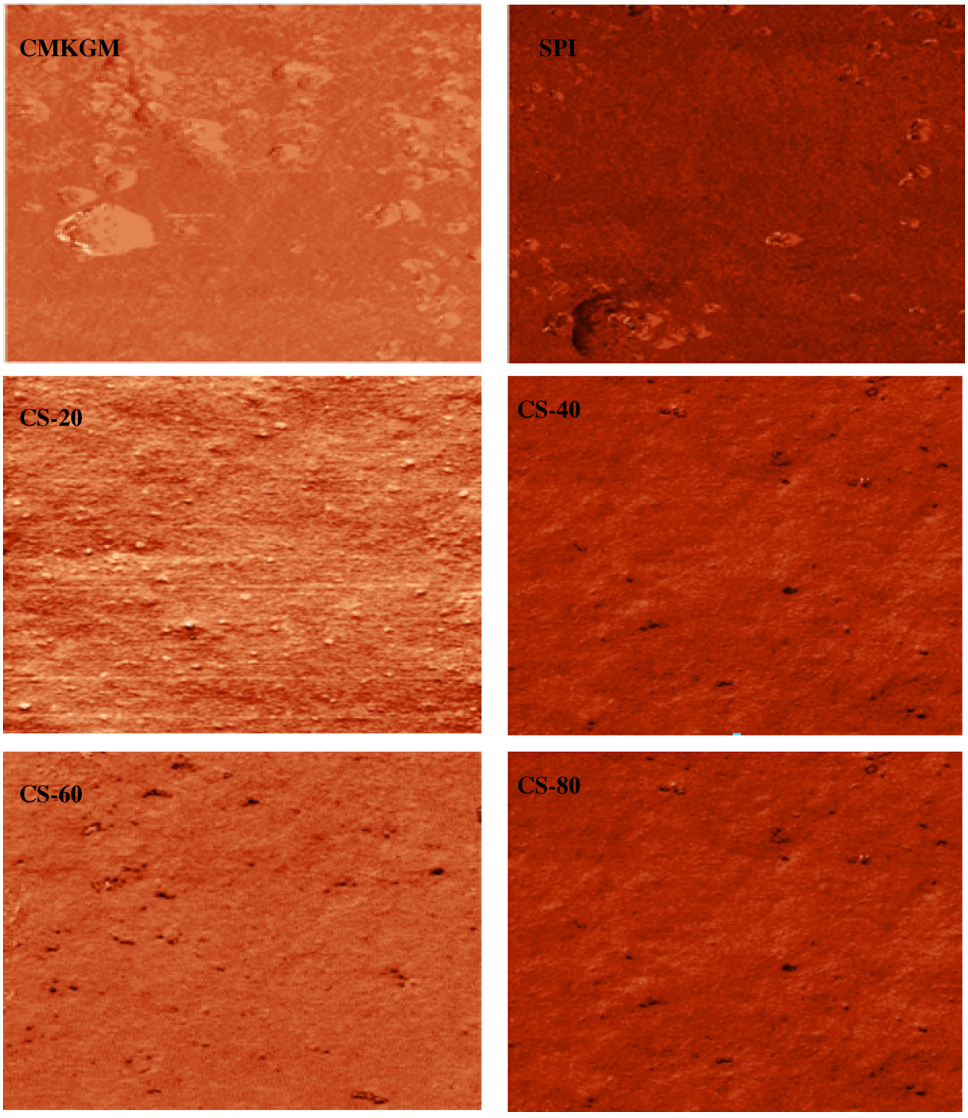

Fig. 9. Typical AFM images of the surface topography of the films. Scan size (5 μm × 5 μm).

3.4.5. *Surface roughness*

AFM images were obtained with the aim of quantifying the impact of active ingredients on the surface topography of the films (Fig. 9). As expected the surface topography of CMKGM and SPI film obtained from SEM images was extremely smooth and homogenous (Fig. 4c). In addition, the topography of the CS-20 and CS-40 films was rough and heterogeneous. The roughness parameters such as *Ra* and *Rq* of films were measured (Table 2). The CS-20 and CS-40 films exhibited high values of *Ra* and *Rq*, with no significant differences ($p > 0.05$). The SPI films had low values of *Ra* (24.2 ± 8.1 nm) and *Rq* (30.7 ± 10.2 nm) in comparison with the other films. The higher the CMKGM content, the lower the roughness. The increasing amount of blisters and depressions formed in the surface of the CMKGM/SPI films as CMKGM content decreased contributed to a higher roughness. These differences in microstructure could be attributed to interactions between CMKGM and SPI

Table 2
Average roughness (*Ra*) and root-mean-square roughness (*Rq*) of the films.

Samples	*Ra* (nm)	*Rq* (nm)
SPI	24.2 ± 8.1^{ab}	30.7 ± 10.2^{ab}
CS-20	54.4 ± 17.3^{a}	70.3 ± 15.3^{a}
CS-40	48.6 ± 12.4^{b}	62.6 ± 14.4^{b}
CS-60	40.1 ± 7.7^{a}	52.3 ± 11.2^{a}
CS-80	33.6 ± 9.6^{c}	46.3 ± 13.8^{c}
CMKGM	33.5 ± 6.1^{b}	47.3 ± 9.6^{b}

Values are means ± standard deviation, $n = 3$. The same letters in a column means no significant differences at $p > 0.05$.

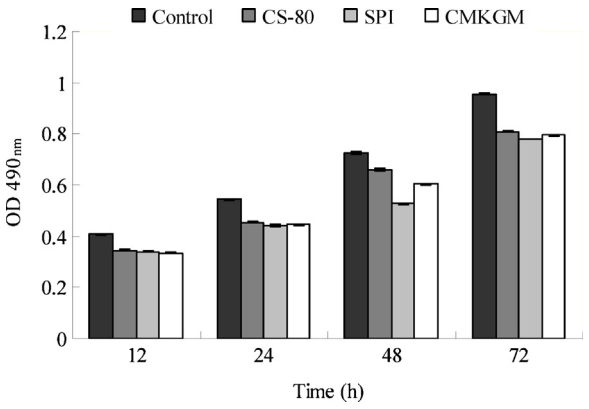

Fig. 10. The absorbance of L929 cells cultured in media without film (control) and with films (CS-80, SPI, and CMKGM) after 12, 24, 48, and 72 h of cell culture.

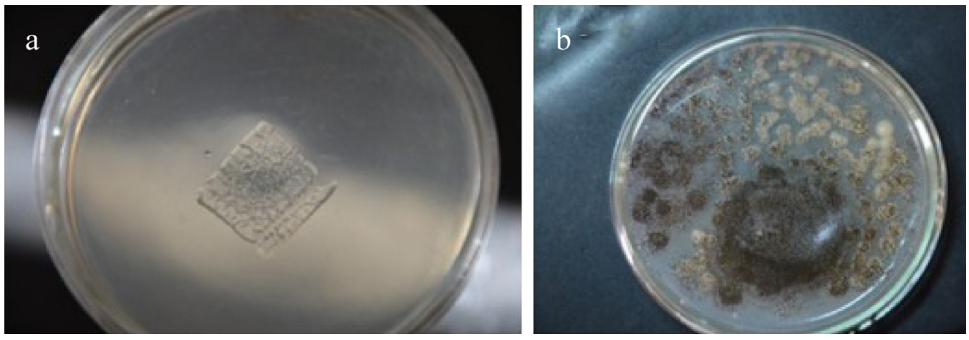

Fig. 11. Growth of *Aspergillus niger* (CGMCC 3.3928) on surface of CMKGM/SPI film. (a) CMKGM/SPI film without *Aspergillus niger*; (b) CMKGM/SPI film with *Aspergillus niger*. The samples were incubated for 15 days at 25 °C.

which gave rise to different types of chain packing that modified the availability of unoccupied volume in the biopolymer matrix. It is also important to consider electrostatic interactions between both types of molecule.

3.4.6. Biocompatibility

With increasing cell incubation time from 12 to 72 h, the proliferation of L929 cells growing in medium with and without film groups increased gradually; the number of cells in media without films was better than that in media in the presence of films (Fig. 10).

After cells cultured in media without film (control) and in the present films (CS-80, SPI, and CMKGM) for 12, 24, 48, and 72 h, the relative cell viability (%), calculated as $OD_{490\,nm}$ in media containing films as the percentage of $OD_{490\,nm}$ in media without films, was 83, 83, and 82%; 83, 81, and 82%; 91, 73, and 83%; 84, 82, and 83%; respectively. The cell viability values were greater than 82%, indicating films posed nearly no toxicity to the L929 cells. The results showed that CMKGM/SPI films have good biocompatibility.

3.4.7. Biodegradability of CMKGM/SPI with A. niger

The growth of *A. niger* was clearly visible on the surface of CMKGM/SPI film (Fig. 11). While, no colony growth during culture period was observed for the CMKGM/SPI film without incubating *A. niger* on the agar surfaces (Fig. 11). So the CMKGM/SPI film can be degraded by the *A. niger*. This result is the similar to films biological degradation, e.g., the extracellular polysaccharide film biological degradation (Alves et al., 2011), the chitosan-graft-polymethylmethacrylate flim (Harish Prashanth, Lakshman, Shamala, & Tharanathan, 2005), and the starch films (Torres, Troncoso, Torres, Díaz, & Amaya, 2011).

4. Conclusion

By blending CMKGM with SPI, interaction between these two biopolymers was established, and blended films showed different physicochemical properties compared to pure CMKGM and SPI films.

The CMKGM/SPI mixture allowed film formation without use of plasticizer. CMKGM/SPI blend films showed higher elongation at break and tensile strength than pure CMKGM and SPI, and the water sensitivity of blend films decreased with increasing CMKGM content. The FTIR data indicated Maillard reactions and hydrogen bonding interactions occurred between CMKGM and SPI. XRD and DSC revealed CMKGM and SPI are compatible. The results of SEM and oxygen permeability confirmed this point microstructurally.

Biopolymer interactions between carboxymethylated konjac glucomannan and soy protein isolate were due to Maillard reactions, hydrogen bond interaction and compatibility in the blend film, leading to the reported change in physicochemical properties.

Acknowledgement

This work was financially supported by National Natural Science Foundation of China (Nos. 31071520, 31271832, and 31301428).

References

Aaslyng, M. D., Larsen, L. M., & Nielsen, P. M. (1999). The influence of maturation on flavor and chemical composition of hydrolyzed soy protein produced by acidic and enzymatic hydrolysis. *Zeitschrift für Lebensmitteluntersuchung und-Forschung A*, *208*(5), 355–361.

Abugoch, L. E., Tapia, C., Villamán, M. C., Yazdani-Pedram, M., & Díaz-Dosque, M. (2011). Characterization of quinoa protein–chitosan blend edible films. *Food Hydrocolloids*, *25*(5), 879–886.

Alves, V. D., Ferreira, A. R., Costa, N., Freitas, F., Reis, M. A., & Coelhoso, I. M. (2011). Characterization of biodegradable films from the extracellular polysaccharide produced by *Pseudomonas oleovorans* grown on glycerol byproduct. *Carbohydrate Polymers*, *83*(4), 1582–1590.

ASTM-D-882-91. (1991). Standard test methods for tensile properties of thin plastic sheeting. In *Annual book of ASTM*. Philadelphia, PA: American Society for Testing & Materials.

Biliaderis, C., Lazaridou, A., & Arvanitoyannis, I. (1999). Glass transition and physical properties of polyol-plasticised pullulan–starch blends at low moisture. *Carbohydrate Polymers*, *40*(1), 29–47.

Chen, J., Li, J., & Li, B. (2011). Identification of molecular driving forces involved in the gelation of konjac glucomannan: Effect of degree of deacetylation on hydrophobic association. *Carbohydrate Polymers*, *86*(2), 865–871.

Chua, M., Chan, K., Hocking, T. J., Williams, P. A., Perry, C. J., & Baldwin, T. C. (2012). Methodologies for the extraction and analysis of konjac glucomannan from corms of Amorphophallus konjac K. Koch. *Carbohydrate Polymers*, *87*(3), 2202–2210.

Debeaufort, F., Voilley, A., & Luu, D. (2009). Biopolymer interactions affect the functional properties of edible films based on agar, cassava starch and arabinoxylan blends. *Journal of Food Engineering*, *90*(4), 548–558.

Denavi, G. A., Pérez-Mateos, M., Añón, M. C., Montero, P., Mauri, A. N., & Gómez-Guillén, M. C. (2009). Structural and functional properties of soy protein isolate and cod gelatin blend films. *Food Hydrocolloids*, *23*(8), 2094–2101.

Di Pierro, P., Chico, B., Villalonga, R., Mariniello, L., Damiao, A. E., Masi, P., et al. (2006). Chitosan-whey protein edible films produced in the absence or presence of transglutaminase: Analysis of their mechanical and barrier properties. *Biomacromolecules*, *7*(3), 744–749.

Du, J., Dai, J., Liu, J. L., & Dankovich, T. (2006). Novel pH-sensitive polyelectrolyte carboxymethyl Konjac glucomannan-chitosan beads as drug carriers. *Reactive and Functional Polymers*, *66*(10), 1055–1061.

Du, X., Li, J., Chen, J., & Li, B. (2012). Effect of degree of deacetylation on physicochemical and gelation properties of konjac glucomannan. *Food Research International*, *46*(1), 270–278.

El-Sherbiny, I. (2009). Synthesis, characterization and metal uptake capacity of a new carboxymethyl chitosan derivative. *European Polymer Journal*, *45*(1), 199–210.

García, M. A., Martino, M. N., & Zaritzky, N. E. (2000). Lipid addition to improve barrier properties of edible starch-based films and coatings. *Journal of Food Science*, *65*(6), 941–944.

GB/T 1038-2000. (2000). *Plastics-film and sheeting-determination of gas transmission-differential pressure method*.

Hägerdal, B., & Martens, H. (1976). Influence of water content on the stability of myoglobin to heat treatment. *Journal of Food Science*, *41*(4), 933–937.

Harish Prashanth, K. V., Lakshman, K., Shamala, T. R., & Tharanathan, R. N. (2005). Biodegradation of chitosan-graft-polymethylmethacrylate films. *International Biodeterioration and Biodegradation*, *56*(2), 115–120.

Hill, C. A., Norton, A., & Newman, G. (2009). The water vapor sorption behavior of natural fibers. *Journal of Applied Polymer Science*, *112*(3), 1524–1537.

Jansson, A., Järnström, L., Rättö, P., & Thuvander, F. (2006). Physical and swelling properties of spray-dried powders made from starch and poly(vinyl alcohol). *Starch–Stärke*, *58*(12), 632–641.
Kobayashi, S., Tsujihata, S., Hibi, N., & Tsukamoto, Y. (2002). Preparation and rheological characterization of carboxymethyl konjac glucomannan. *Food Hydrocolloids*, *16*(4), 289–294.
Kumar, P., Sandeep, K., Alavi, S., Truong, V. D., & Gorga, R. (2010). Preparation and characterization of bio-nanocomposite films based on soy protein isolate and montmorillonite using melt extrusion. *Journal of Food Engineering*, *100*(3), 480–489.
Kyung Kim, J., Jo, C., Jin Park, H., & Woo Byun, M. W. (2008). Effect of gamma irradiation on the physicochemical properties of a starch-based film. *Food Hydrocolloids*, *22*(2), 248–254.
Mariani, P., Allganer, K., Oliveira, F., Cardoso, E., & Innocentini-Mei, L. (2009). Effect of soy protein isolate on the thermal, mechanical and morphological properties of poly(ε-caprolactone) and corn starch blends. *Polymer Testing*, *28*(8), 824–829.
Martins, J. T., Cerqueira, M. A., Bourbon, A. I., Pinheiro, A. C., Souza, B. W. S., & Vicente, A. A. (2012). Synergistic effects between κ-carrageenan and locust bean gum on physicochemical properties of edible films made thereof. *Food Hydrocolloids*, *29*(2), 280–289.
Mauri, A. N., & Añón, M. C. (2006). Effect of solution pH on solubility and some structural properties of soybean protein isolate films. *Journal of the Science of Food and Agriculture*, *86*(7), 1064–1072.
Neamnark, A., Sanchavanakit, N., Pavasant, P., Bunaprasert, T., Supaphol, P., & Rujiravanit, R. (2007). In vitro biocompatibility evaluations of hexanoyl chitosan film. *Carbohydrate Polymers*, *68*(1), 166–172.
Niu, C., Wu, W., Wang, Z., Li, S., & Wang, J. (2007). Adsorption of heavy metal ions from aqueous solution by crosslinked carboxymethyl konjac glucomannan. *Journal of Hazardous Materials*, *141*(1), 209–214.
Park, S., Hettiarachchy, N., & Were, L. (2000). Degradation behavior of soy protein-wheat gluten films in simulated soil conditions. *Journal of Agricultural and Food Chemistry*, *48*(7), 3027–3031.
Pei, Y., Yang, J., Liu, P., Xu, M., Zhang, X., & Zhang, L. (2013). Fabrication, properties and bioapplications of cellulose/collagen hydrolysate composite films. *Carbohydrate Polymers*, *92*(2), 1752–1760.
Rhim, J. W. (2004). Increase in water vapor barrier property of biopolymer-based edible films and coatings by compositing with lipid materials. *Food Science and Biotechnology*, *13*(4), 528–535.
Rhim, J. W. (2007). Mechanical and water barrier properties of biopolyester films prepared by thermo-compression. *Food Science and Biotechnology*, *16*(1), 62–66.
Roos, Y., & Karel, M. (2006). Plasticizing effect of water on thermal behavior and crystallization of amorphous food models. *Journal of Food Science*, *56*(1), 38–43.
Shand, P., Ya, H., Pietrasik, Z., & Wanasundara, P. (2007). Physicochemical and textural properties of heat-induced pea protein isolate gels. *Food Chemistry*, *102*(4), 1119–1130.
Siracusa, V., Rocculi, P., Romani, S., & Rosa, M. D. (2008). Biodegradable polymers for food packaging: A review. *Trends in Food Science and Technology*, *19*(12), 634–643.
Song, F., Tang, D. L., Wang, X. L., & Wang, Y. Z. (2011). Biodegradable soy protein isolate-based materials: A review. *Biomacromolecules*, *12*(10), 3369–3380.
Su, J. F., Huang, Z., Liu, K., Fu, L. L., & Liu, H. R. (2007). Mechanical properties, biodegradation and water vapor permeability of blend films of soy protein isolate and poly(vinyl alcohol) compatibilized by glycerol. *Polymer Bulletin*, *58*(5), 913–921.
Su, J. F., Huang, Z., Yuan, X. Y., Wang, X. Y., & Li, M. (2010). Structure and properties of carboxymethyl cellulose/soy protein isolate blend edible films crosslinked by Maillard reactions. *Carbohydrate Polymers*, *79*(1), 145–153.
Tang, C. H., Jiang, Y., Wen, Q. B., & Yang, X. Q. (2005). Effect of transglutaminase treatment on the properties of cast films of soy protein isolates. *Journal of Biotechnology*, *120*(3), 296–307.
Tang, R., Du, Y., Zheng, H., & Fan, L. (2003). Preparation and characterization of soy protein isolate–carboxymethylated konjac glucomannan blend films. *Journal of Applied Polymer Science*, *88*(5), 1095–1099.
Torres, F. G., Troncoso, O. P., Torres, C., Díaz, D. A., & Amaya, E. (2011). Biodegradability and mechanical properties of starch films from Andean crops. *International Journal of Biological Macromolecules*, *48*(4), 603–606.
Wang, C., Li, B., & Xie, B. J. (2005). Effect of deacetylation in course of konjac glucomannan carboxy methylation and structure characterization of the products. *Scientia Agricultura Sinica*, *38*(10), 2090–2095.
Wihodo, M., & Moraru, C. I. (2012). Physical and chemical methods used to enhance the structure and mechanical properties of protein films. A review. *Journal of Food Engineering*, *114*(3), 292–302.
Xiao, C., Liu, H., Lu, Y., & Zhang, L. (2001). Characterization of poly(vinylpyrrolidone)–konjac glucomannan blend films. *Journal of Applied Polymer Science*, *81*(5), 1049–1055.
Yu, L., Dean, K., & Li, L. (2006). Polymer blends and composites from renewable resources. *Progress in Polymer Science*, *31*(6), 576–602.
Zhan, X. H., Chen, G. F., Li, W. F., Zhou, J., Huang, J., & Jiang, F. T. (2006). Preparation and property of soy protein isolate/carboxymethylated konjac glucomannan blend film. *Science and Technology of Food Industry*, *27*(8), 144–145.
Zhang, J., Mungara, P., & Jane, J. (2001). Mechanical and thermal properties of extruded soy protein sheets. *Polymer*, *42*(6), 2569–2578.
Zhang, M., Song, F., Wang, X. L., & Wang, Y. Z. (2012). Development of soy protein isolate/waterborne polyurethane blend films with improved properties. *Colloids and Surfaces B: Biointerfaces*, *100*, 16–21.
Zhou, J., Wang, C., Zhan, X. H., Li, W. F., Chen, G. F., Huang, J., et al. (2006). Effect of sodium acetate on carboxy methyl action of konjac glucomannan. *Food Research and Development*, *27*(7), 51–53.